HHS Public Access

Author manuscript

AJR Am J Roentgenol. Author manuscript; available in PMC 2021 February 01.

Published in final edited form as:

AJR Am J Roentgenol. 2020 February ; 214(2): 362–369. doi:10.2214/AJR.19.21152.

Assessment of Response to Neoadjuvant Therapy Using CT Texture Analysis in Patients With Resectable and Borderline Resectable Pancreatic Ductal Adenocarcinoma

Amir A. Borhani[1], **Rohit Dewan**[1,2], **Alessandro Furlan**[1], **Natalie Seiser**[3,4], **Amer H. Zureikat**[3], **Aatur D. Singhi**[5], **Brian Boone**[3,6], **Nathan Bahary**[7], **Melissa E. Hogg**[3,8], **Michael Lotze**[9], **Herbert J. Zeh III**[3,10], **Mitchell E. Tublin**[1]

[1]Department of Radiology, Division of Abdominal Imaging, University of Pittsburgh Medical Center, Ste 200 E Wing, 200 Lothrop St, Pittsburgh, PA 15213.

[2]Present address: Department of Radiological Sciences, David Geffen School of Medicine at UCLA, Los Angeles, CA.

[3]Department of Surgery, Division of Gastrointestinal Surgical Oncology, University of Pittsburgh School of Medicine, Pittsburgh, PA.

[4]Present address: Transplant and Hepato-Pancreato-Biliary (HPB) Institute, St. Vincent Medical Center, Los Angeles, CA.

[5]Department of Pathology, University of Pittsburgh School of Medicine, Pittsburgh, PA.

[6]Present address: Department of Surgery, Division of Surgical Oncology, West Virginia University, Morgantown, WV.

[7]Department of Medicine, Division of Hematology/Oncology, University of Pittsburgh School of Medicine, Pittsburgh, PA.

[8]Present address: Department of Surgery, NorthShore University Hospital, Evanston, IL.

[9]Department of Surgery, University of Pittsburgh School of Medicine, Pittsburgh, PA.

[10]Present address: Department of Surgery, University of Texas Southwestern Medical Center, Dallas, TX.

Abstract

OBJECTIVE.—The goal of this study was to assess the correlation between CT-derived texture features of pancreatic ductal adenocarcinoma (PDAC) and histologic and biochemical markers of response to neoadjuvant treatment as well as disease-free survival in patients with potentially resectable PDAC.

SUBJECTS AND METHODS.—Thirty-nine patients completed this prospective study protocol between November 2013 and December 2016. All patients received neoadjuvant chemotherapy,

Address correspondence to A. A. Borhani (borhaniaa@upmc.edu).

Based on presentations at the Radiological Society of North America 2017 annual meeting, Chicago, IL; Society of Abdominal Radiology 2018 annual meeting, Scottsdale, AZ; and Society of Surgical Oncology 2018 annual meeting, Chicago, IL.

underwent surgical resection, and had histologic grading of tumor response. Similar CT protocol was used for all patients. Pancreatic (late arterial) phase of pre- and posttreatment CT scans were evaluated. Histogram analysis and spatial-band-pass filtration were used to extract textural features. Correlation between textural parameters, histologic response, biochemical response, and genetic mutations was assessed using Mann-Whitney test, chi-square analysis, and multivariate logistic regression. Association with disease-free survival was assessed using Kaplan-Meier method and Cox model.

RESULTS.—Pretreatment mean positive pixel (MPP) at fine- and medium-level filtration, pretreatment kurtosis at medium-level filtration, changes in kurtosis, and pretreatment tumor SD were statistically different between patients with no or poor histologic response and favorable histologic response ($p < 0.05$). Changes in skewness and kurtosis at medium-level filtration significantly correlated with biochemical response ($p < 0.01$). On the basis of multivariate analysis, patients with higher MPP at pretreatment CT were more likely to have favorable histologic response (odds ratio, 1.06; 95% CI, 1.002–1.12). The Cox model for association between textural features and disease-free survival was statistically significant ($p = 0.001$).

CONCLUSION.—Textural features extracted from baseline pancreatic phase CT imaging of patients with potentially resectable PDAC and longitudinal changes in tumor heterogeneity can be used as biomarkers for predicting histologic response to neoadjuvant chemotherapy and disease-free survival.

Keywords

CT; neoadjuvant chemotherapy; pancreatic adenocarcinoma; pancreatic cancer; texture analysis

Pancreatic ductal adenocarcinoma (PDAC) is the fourth most common malignancy in the United States [1]. Despite recent improvements in tumor detection and medical and surgical management, the prognosis for patients even with potentially surgically resectable disease remains dismal [2]. Recently, several new effective systemic chemotherapy regimens for PDAC have been described in the metastatic setting [3]. This has led to an increased enthusiasm for preoperative chemotherapy before attempted resection [4]. This experience has, however, identified a clinical dilemma not previously well described, whereby the response to preoperative chemotherapy in the primary pancreatic tumor cannot be reliably predicted on the basis of standard criteria. PDAC is typically an infiltrating, relatively hypovascular tumor, so common imaging biomarkers used in other solid tumors, such as size and vascularity, are not helpful. Cancer antigen (CA) 19–9 lacks sensitivity and cannot be used as the sole criterion for assessment of treatment response [5, 6]. Several groups have even advocated for surgical exploration and attempted resection of all patients receiving preoperative therapy in the absence of reliable markers of response [4, 7], which is costly and can result in increased morbidity to patients receiving nontherapeutic laparotomy. A noninvasive imaging marker that evaluates tumor aggressiveness and assesses the likelihood of treatment response is critically necessary and would have a dramatic and immediate impact on the management of these patients.

Tumor heterogeneity is a well-described image-based feature reflecting the tumor microenvironment that correlates with tumor hypoxia and angiogenesis [8]. Computer-based

quantitative texture analysis is an emerging postprocessing tool to extract additional features from conventional imaging studies. Recent studies have suggested an association between tumor texture, tumor molecular biology, and survival in different types of cancer including lung, breast, colorectal, esophageal, and renal cancers [8–12]. Recent studies showed how CT-derived texture features correlated with overall survival in patients with PDAC [13–15]. The purpose of this study is to assess the correlation between CT-derived texture features of PDAC and histopathologic and biochemical markers of response to neoadjuvant treatment in patients with potentially resectable PDAC. Additionally, the role of texture analysis as a biomarker for disease-free survival was also investigated.

Subjects and Methods

Patient Cohort

The imaging component of this study was an adjunct of a prospective randomized study approved by the institutional review board of the University of Pittsburgh Cancer Institute that evaluated the efficacy of neoadjuvant therapy (gemcitabine and paclitaxel alone or in combination with the autophagy inhibitor hydroxychloroquine) in patients with resectable and borderline resectable, histologically proven PDAC. Detailed inclusion and exclusion criteria and the trial protocol are summarized in Appendix 1. Informed consent was obtained. Sixty-three patients completed the protocol between November 2013 and December 2016 and were evaluable for both primary and secondary endpoints. After CT examinations were reviewed, 24 patients were excluded from image analysis for various reasons: small (< 1 cm) size of tumor (n = 8), isoenhancement and inconspicuity of tumor (n = 1), predominantly cystic nature of tumor (n = 1), presence of concurrent pancreatic inflammation (n = 1), and poor image quality (n = 1). Patients who had their imaging studies performed at outside facilities with differing CT acquisition parameters were also excluded (n = 12). Thirty-nine patients were thus included in the final image analysis (Fig. 1). The patients' age, sex, neoadjuvant chemotherapy regimen, tumor size at presentation, tumor location, histologic grade of tumor, tumor stage at presentation, genetic mutation, type of surgery, recurrence, and disease-free survival were recorded.

CT Imaging Technique

All studies were performed on a 64-MDCT scanner (VCT or Optima, GE Healthcare) using a triphasic pancreatic mass protocol. The CT examination consisted of an initial unenhanced helical acquisition through the abdomen (120 kVp; noise index, 37.59; acquisition thickness, 0.625 × 0.625 mm; automatic tube current, 100–550 mA; pitch, 1.375; rotation time, 0.6 s; detector coverage, 40 mm). A dose of 100 mL, 125 mL, or 150 mL of IV iodinated contrast agent (iopamidol, 370 mg I/mL concentration, Bracco Diagnostics) was administered on the basis of the patient's weight category (< 140 lb [63.5 kg], 140–240 lb [63.5–108.9 kg], > 240 lb [108.9 kg]) at 5 mL/s rate using a power injector. Contrast-enhanced CT images were acquired during the late arterial (pancreatic) phase (120 kVp; noise index, 25; acquisition thickness, 0.625 × 0.625 mm; automatic tube current, 100–650 mA; pitch, 0.984; rotation time, 0.6 s; detector coverage, 40 mm) and venous phase (120 kVp; noise index, 25; acquisition thickness, 0.625 × 0.625 mm; automatic tube current, 100–650 mA; pitch, 1.375; rotation time, 0.6 s; detector coverage, 40 mm). SmartPrep software (version 15HW25.x, GE

Healthcare) was used to time the administration of contrast agent for the late hepatic arterial phase: imaging was initiated 20 seconds after a threshold enhancement of 100 HU was achieved in the suprarenal aorta. Venous phase images were then obtained 50 seconds after the acquisition of the late arterial phase images. Axial contrast-enhanced images were reconstructed at 2.5-mm thickness with 2.5-mm interval using a soft-tissue algorithm and with application of 30% adaptive statistical iterative reconstruction.

CT Image Analysis

The CT examinations were reviewed in retrospective fashion by a fellowship-trained abdominal radiologist with 6 years of experience in advanced pancreatic imaging. The studies were anonymized and exported to a dedicated research workstation. The reader was blinded to clinical, laboratory, and histopathologic data at the time of image analysis. All three phases of CT examinations were available and reviewed for better delineation of tumor from the adjacent structures. Late arterial (pancreatic) phase images were used for texture analysis: these images were used because of the typically greater contrast resolution and tumor conspicuity of PDAC during the late arterial phase. Images were viewed and analyzed on a commercially available research platform (TexRAD, version 3.9, Feedback Plc). The slice with largest cross section of tumor was chosen for image analysis. A free-hand polygonal ROI was drawn inside the pancreatic mass (Fig. 2). The pretreatment CT (baseline CT before initiation of neoadjuvant chemotherapy) and posttreatment CT (the study performed after completion of neoadjuvant chemotherapy and immediately before surgery) images were reviewed and analyzed sequentially so that the ROIs were similar in size and location.

Texture Analysis Technique

The research platform used for this study performs in-plane filtration of images using a Laplacian of gaussian spatial-band-pass filter to extract and enhance textural features at fine (2-mm spatial scale), medium (3- and 4-mm spatial scale), and coarse (5- and 6-mm spatial scale) levels, as previously described [16, 17]. For each ROI, first-order statistical features of the gray-level histograms of both filtered and unfiltered images were quantified. Mean, SD (degree of dispersion), mean positive pixel value (MPP), kurtosis (flatness), and skewness (asymmetry) of the pixel-distribution histogram were calculated for filtered and unfiltered images. MPP reflects the mean brightness of positive values after filtration, whereas kurtosis and skewness describe the shape of the histogram. In addition, entropy (which is an index of non-uniformity and heterogeneity) was calculated for each image (on the basis of the formula described in [16]). Textural parameters of filtered and unfiltered images were extracted from both pre- and posttreatment CT studies. The absolute difference (the difference between posttreatment value and pretreatment value) and percentage difference (the difference between posttreatment value and pretreatment value, divided by the pretreatment value) between texture parameters of pre- and posttreatment CT studies were also calculated.

Laboratory Analysis

All patients had a serial serum CA19–9 level measured before and after neoadjuvant chemotherapy. The blood assay was performed in the same laboratory using the same

reference standards. A threshold of 37 U/mL was used as the definition of an abnormal CA19–9 level.

Surgical Specimen

All patients underwent surgical resection for PDAC via pancreaticoduodenectomy, distal pancreatectomy, or Appleby procedure depending on the location of the tumor. On gross evaluation, the entire PDAC specimen was submitted for histopathologic evaluation. For cases in which a grossly identifiable mass was not present, the entire pancreas was submitted in a systematic fashion. H and E-stained slides were evaluated by a single expert pancreatobiliary pathologist who was not aware of an individual patient's treatment arm. Treatment response was categorized using the Evans grading system (Table 1). In addition to Evans grade, additional pertinent pathologic assessments included histologic grade, margin status, stage, and lymph node status. Immunohistochemical evaluation of *SMAD4* expression was also performed. Staging was using the 7th edition of the American Joint Committee on Cancer (AJCC) manual [18].

Statistical Analysis

Continuous variables were summarized using mean, median, range, and SD; categoric variables were summarized using frequency and percentages. Chi-square analyses were used to compare categoric data, whereas continuous variables were analyzed using a Mann-Whitney nonparametric *U* test. Evans grades I and IIA were considered as nonfavorable responses and grades IIB-IV were considered favorable treatment responses. A biochemical response was defined as greater than a 50% decrease in CA19–9 level after neoadjuvant chemotherapy in patients with abnormal initial CA19–9 level. Associations between textural features, treatment response (favorable vs nonfavorable), biochemical response, and genetic mutations were tested with a Mann-Whitney nonparametric *U* test. Multivariate logistic regression was performed to examine possible predictors of a favorable outcome. Factors that achieved a *p* value of less than 0.05 from the Mann-Whitney *U* tests were entered into the models. Textural parameters that were found to be highly correlated with each other (on the basis of Pearson correlation coefficient) were not entered into the models at the same time. Results were presented as odds ratios (OR) with 95% CIs. Finally, the association between textural features, biochemical response, histologic response, and disease-free survival were assessed using the Kaplan-Meier method (log-rank test) and Cox model (for binary and continuous variables, respectively).

A *p* value of less than 0.05 was considered statistically significant. Bonferroni correction was not applied for multiple comparisons given the small sample size. Statistical analysis was performed using statistical software (SPSS Statistics for Macintosh, version 25, IBM).

Results

Study Population

The final study population consisted of 39 patients (20 men, 19 women; median age, 67 years) with 39 lesions (Table 2). Tumor distribution was pancreatic head (*n* = 32; 82%), body (*n* = 4; 10%), and tail (*n* = 3; 8%). Mean tumor size was 2.9 cm (range, 1–5 cm). Four

patients (10%) had cancer staged as AJCC stage IB, 10 (26%) as IIA, and 25 (64%) as IIB on the basis of imaging studies (CT and endoscopic ultrasound) at presentation. All patients received two cycles of neoadjuvant chemotherapy with gemcitabine and paclitaxel, with or without hydroxychloroquine. Seventeen patients (44%) also received hydroxychloroquine. None of the patients received preoperative radiation.

Resections performed included pancreaticoduodenectomy (n = 32; 82%), distal pancreatectomy (n = 5; 13%), and Appleby procedure (n = 2; 5%). In 28 patients (72%), a margin negative (R0) resection was achieved. Histologic grade was moderately differentiated (n = 30; 77%), poorly differentiated (n = 8; 21%), and undifferentiated (n = 1; 3%). Twenty-two (56%) patients had loss of *SMAD4* nuclear expression. Evans grading of pathologic response was categorized as grade I for 11 (28%) cases, IIa for 17 (44%), IIb for nine (23%), and III for two (5%) cases. CA19–9 was not a marker in nine (23%) patients. In patients in whom CA19–9 was a marker, mean pretreatment and posttreatment serum CA19–9 levels were 865.6 U/mL and 97.6 U/mL, respectively. Among the 30 patients who had an elevated CA19–9 level, 25 (83%) had a biochemical response. Twenty-five of the 39 patients (64%) had recurrence with mean time to recurrence of 10.5 months (range, 1–33 months), and 15 patients (38%) died during the study period. One patient died during the immediate post-operative period; the remainder of the deaths occurred as a result of disease recurrence. Mean disease-free survival by the time of completion of the study was 14.1 months (range, 0–38 months). The association between patient characteristics and pathologic response is summarized in Table 2. Chemotherapy regimen (gemcitabine and paclitaxel vs gemcitabine and paclitaxel with hydroxychloroquine) was the only clinical parameter that correlated with pathologic response.

Texture Analysis

The median values of different textural features as well as results of nonparametric tests are summarized in Table 3. When Evans pathologic response was redefined as a dichotomous categoric variable (Evans grade I-IIA [nonfavorable] response vs Evans grade IIB-IV [favorable] response), pretreatment tumor MPP at fine- and medium-level filtration (MPP-2 and MPP-4), pretreatment kurtosis at medium-level filtration (Kurtosis-3), changes between tumor kurtosis before and after treatment on unfiltered images (Dkurtosis), and pretreatment tumor SD (SD-2) showed statistically significant differences between the two groups (p = 0.009, 0.021, 0.034, 0.032, 0.049, respectively).

Changes between tumor skewness and kurtosis before and after treatment at medium-level filtration (Dskewness-4 and Dkurtosis-4) were significantly correlated with biochemical response (p = 0.007, Mann-Whitney U = 6; p = 0.01, Mann-Whitney U = 7; respectively) (Fig. 3). No significant association between textural features, tumor grade, and genetic mutation (loss of *SMAD4*) was observed.

Logistic Regression Analysis

On the basis of the univariate analyses, the variables found to be associated with a favorable outcome included chemotherapy regimen, MPP-2, MPP-4, Kurtosis-3, and SD-2. Because of the high correlation between MPP-2 with MPP-4 and SD-2 (r = 0.43, p = 0.006; r = 0.49, p =

0.001; respectively), those variables were not entered into the model at the same time. Results from the multivariable models are presented in Table 4. Multivariate analysis showed that those receiving the chemotherapy regimen with gemcitabine and paclitaxel with hydroxychloroquine were 11.3 (95% CI, 1.98–63.95) times more likely to have a favorable outcome than those on just gemcitabine and paclitaxel. Higher MPP-4 (OR, 1.06; 95% CI, 1.002–1.11) and MPP-2 (OR, 1.10; 95% CI, 1.02–1.21) were also found to be significant predictors. After adjusting for chemotherapy regimen, those with a higher MPP-4 were 1.06 (95% CI, 1.002–1.12) times more likely to have a favorable outcome.

Disease-Free Survival

Kaplan-Meier method with log-rank test showed a statistically significant difference in disease-free survival on the basis of biochemical response ($\chi^2 = 5.429$, $p = 0.02$) and pathologic response ($\chi^2 = 3.945$, $p = 0.047$) (Fig. 4).

The Cox model was used to assess the association between the selected textural features (the ones that showed best correlation with the response on nonparametric tests, i.e., pretreatment MPP-2, MPP-4, and Kurtosis-3) and disease-free survival. The model based on Cox model was statistically significant ($\chi^2 = 17.065$, $p = 0.001$) and demonstrated a statistically significant hazard ratio of 1.099 (95% CI, 1.037–1.165; $p = 0.002$) for Kurtosis-3.

Discussion

Results of our study suggest that CT-derived tumor textural features may have a relationship with tumor response to neoadjuvant chemotherapy. Assessment of pancreatic tumor response to chemotherapy using conventional imaging methods remains challenging [19]. Several studies have found that size of the primary pancreatic tumor cannot be used as a reliable imaging marker of potential treatment response [4, 20]. Despite significant treatment response at the histologic level, there might be no appreciable change in size of PDAC and the degree of vascular involvement (Fig. 2). CA19–9 is the only serum tumor marker currently used for assessment of response in these patients that lacks sensitivity. In up to 22% of patients, however, CA19–9 level is not elevated [6], so this antigen cannot be used as a marker in this subset of patients.

Recent meta-analyses and small prospective trials have shown that patients who receive neoadjuvant chemotherapy have an overall higher R0 resection rate, fewer positive lymph nodes, and higher disease-free survival [21–23]. Repeat imaging and CA19–9 assay after completion of neoadjuvant chemotherapy serve as guides for risk stratification and patient selection for curative surgery. Our study suggests that quantitative parameters of tumor heterogeneity on CT can be used as imaging biomarkers of tumor response to chemotherapy. Changes in tumor kurtosis between pre- and posttreatment CT studies correlated with pathologic response and likely reflected treatment-related changes in tumor histology. Moreover, MPP on the baseline pretreatment CT study alone also correlated with pathologic response. We hypothesize that the baseline texture profile of pancreatic tumor reflects the stromal-tumor interactions and the tumor microenvironment beyond tumor grade. These factors, such as tumor vascularity and oxygenation, could in turn affect the delivery and efficacy of chemotherapeutic agents to tumoral cells and have an impact on neoadjuvant

response. A correlation between tumor heterogeneity and tumor angiogenesis has been shown in other tumors [8]. MPP best predicted neoadjuvant response in our study; it is affected by the number of enhancing pixels and hence is a product of tumor vascularity. Patients with favorable responses in our study had higher MPP values, denoting more vascularity. Two recent studies of patients with PDAC also showed that lower attenuation of tumors at baseline venous phase CT were associated with a worse prognosis and earlier recurrence [14, 24], perhaps because of poor delivery of chemotherapeutic agents to tumor cells. Notably, the mean attenuation of the tumor in our study was not different between responders and nonresponders. This could be because we used late-arterial phase imaging for analysis rather than venous phase.

Patients in our cohort were randomized into two treatment arms: gemcitabine and paclitaxel with or without hydroxychloroquine. The OR of pathologic response was higher in patients who received hydroxychloroquine. The baseline CT textural features, however, were found to be predictors of pathologic response independent of treatment. The textural features at baseline CT also performed well for predicting disease-free survival, a finding confirming observations reported by other groups [14, 15, 25].

Our study differs from published reports exploring heterogeneity of PDAC [13–15, 25]. To our knowledge, ours is the only study that uses pathologic response as the primary clinical endpoint. Although overall survival and disease-free survival are affected by many patient- and treatment-related factors, pathologic response reflects the direct interaction between tumor and chemotherapeutic agents. Histologic grading of residual carcinoma following treatment (such as Evans grading of tumor response) has been found to predict patient outcome [26]. Our cohort consisted of a relatively homogeneous group of patients with resectable and borderline resectable lesions with similar treatment regimens and controlled surgical and pathologic approaches. Unlike previous studies, we used late-arterial (pancreatic) phase CT for better delineation and more accurate segmentation of the lesion. Our computerized texture analysis method was also different from those used by the other groups, yielding different parameters and allowing different filtration levels.

Recent studies have proposed other promising imaging biomarkers for assessment of response and survival in PDAC. Wang et al. [27] on patients with advanced PDAC found that apparent diffusion coefficient and FDG PET-derived metabolic indexes can be used to predict response to chemotherapy and the overall survival. The study by Garces-Descovich et al. [28] on patients with different stages of PDAC found that patients with metastatic disease had significantly lower mean apparent diffusion coefficient values. Further studies are required to confirm these results and show the role of these markers for assessment of response to neoadjuvant chemotherapy.

We recognize several limitations of our study. The main limitation is the unavoidable risk of data overfitting due to the small sample size and numerous extracted texture parameters. Cross validation, splitting of data into training and testing sets, and Bonferroni correction were not attempted given the small sample size and preliminary nature of the study. This study is designed to serve as a proof of concept for future large-cohort validation studies.

A second limitation is that the largest cross section of the tumor was used for texture analysis rather than analyzing the entire tumor volume. Although volumetric assessment of the entire tumor may provide more information, some studies showed similar results can be obtained when the largest cross-sectional area is used [29]. We were not technically able to perform 3D texture analysis with our platform and method. Additionally, given the inherent infiltrative nature of the tumor, confident segmentation of the entire volume of the lesion would not have been possible in many cases. We believe that tumor texture on the largest cross section is a realistic estimate of the entire tumor texture because coarse heterogeneity is uncommon with pancreatic adenocarcinoma.

A third limitation is that extracted textural features are affected by CT acquisition techniques, phase of enhancement, and the texture analysis method [30]. All the patients in our cohort had similar imaging protocols with identical acquisition parameters. The texture analysis software used for this study is commercially available, and the method is reproducible. The results of this study, however, might not be applicable to other cohorts with different phases of contrast enhancement or with drastically different scan parameters.

Finally, assessment of the Evans grade of pathologic response as a surrogate endpoint is subjective and imprecise, which may result in interobserver variability. All pancreatectomy specimens were reviewed by a single expert pancreatic pathologist. Additionally, to minimize subjective variability in pathologic assessment, we redefined the Evans ordinal grades as a binary categoric variables. We defined Evans grades IIb-IV (i.e., > 50% tumoral cell destruction) as a favorable response to mirror what is considered a response in other solid tumor-response evaluation systems.

The results of this study suggest that textural features extracted from baseline late-arterial (pancreatic) phase CT imaging of patients with resectable and borderline resectable pancreatic adenocarcinoma and longitudinal changes in tumor heterogeneity can be used as imaging biomarkers for predicting pathologic response to neoadjuvant chemotherapy and disease-free survival. MPP values at baseline CT were features with the strongest correlation. These findings shed light on novel ways to gauge tumor response to chemotherapy and warrant further investigation.

Conclusion

Quantified parameters of tumor texture extracted from baseline late-arterial (pancreatic) phase CT images of patients with resectable and borderline resectable pancreatic adenocarcinoma as well as the longitudinal changes in tumor heterogeneity are promising imaging biomarkers for predicting pathologic response to neoadjuvant chemotherapy and predicting disease-free survival. These findings, however, need to be confirmed and validated in larger cohorts.

Acknowledgments

We thank Kristine Ruppert and Hersh Sagreiya for help with statistical analysis.

A. Furlan has received grant support from GE Healthcare. M. E. Hogg has received grant support from SAGES and Intuitive Robotic Surgery.

Supported in part by the National Pancreas Foundation and grants RO1-CA181450-01 and UL1TR001857 from the National Institutes of Health.

APPENDIX 1:: Clinical Trial Protocol

The trial was approved by the University of Pittsburgh Cancer Institute protocol review committee and institutional review board and was registered with clinicaltrials.gov (clinicaltrials.gov/show/NCT01128296). Patients were considered eligible if they met National Comprehensive Cancer Network criteria for resectable or borderline resectable on contrast-enhanced CT of the chest, abdomen, and pelvis using a pancreas mass protocol. Endoscopic ultrasound biopsy and histologic confirmation of malignancy was required. Subjects could not have received any prior therapy for their cancer and had to have adequate hepatic, renal, cardiovascular, and pulmonary reserves to allow both chemotherapy and surgical extirpation. Subjects with porphyria, active psoriasis, or history of interstitial lung disease were also excluded. Patients were then randomized to receive two cycles of gemcitabine and nab-paclitaxel (1000 mg/m^2 and 125 mg/m^2, respectively, on days 1, 8, and 15) with (PGH) or without (PG) hydroxychloroquine (600 mg twice daily) from day 1 through the evening before planned surgical extirpation. Subjects were restaged with a helical CT scan 14 days after the last dose of chemotherapy and before surgery. Surgical exploration and pancreatectomy were then performed if technically feasible and all toxicities had resolved. Pathologic specimens were preserved, and the entire tumor was submitted for evaluation. Six to 10 weeks after successful surgical removal of their tumor, subjects were free to pursue standard-of-care adjuvant therapy options at the discretion of their treating physician. A subject was deemed evaluable if they had received at least one cycle of chemotherapy and at least 80% of the expected hydroxychloroquine doses and they underwent successful surgical extirpation of their disease. The racial, sex, and ethnic characteristics of the subject population reflect the demographics of Pittsburgh and the surrounding area. One hundred twenty subjects signed informed consent between November 2014 and March 2017. There were 22 screen failures. Ninety-eight subjects were randomized to either the PGH or PG arms. Fifteen subjects (28%) in the PGH arm and 12 (26%) in the PG arm did not complete the protocol requirements to be considered for the primary end point. Reasons for attrition were disease progression (5% PGH vs 8% PG), subject preference (10% PGH vs 7% PG), and regimen limiting adverse toxicity (13% PGH vs 11% PG). Sixty-three subjects completed the trial and were evaluable for the primary and secondary endpoints. Of the subjects who did not complete the protocol for reasons other than disease progression, all but six underwent surgical resection.

References

1. Jemal A, Siegel R, Xu J, Ward E. Cancer statistics, 2010. CA Cancer J Clin 2010; 60:277–300 [PubMed: 20610543]
2. Garcea G, Dennison AR, Pattenden CJ, Neal CP, Sutton CD, Berry DP. Survival following curative resection for pancreatic ductal adenocarcinoma: a systematic review of the literature. JOP 2008; 9:99–132 [PubMed: 18326920]
3. Muñoz Martín AJ, Adeva J, Martínez-Galán J, Reina JJ, Hidalgo M. Pancreatic ductal adenocarcinoma: metastatic disease. Clin Transl Oncol 2017; 19:1423–1429 [PubMed: 28623515]

4. Ferrone CR, Marchegiani G, Hong TS, et al. Radiological and surgical implications of neoadjuvant treatment with FOLFIRINOX for locally advanced and borderline resectable pancreatic cancer. Ann Surg 2015; 261:12–17 [PubMed: 25599322]
5. Locker GY, Hamilton S, Harris J, et al. ASCO. ASCO 2006 update of recommendations for the use of tumor markers in gastrointestinal cancer. J Clin Oncol 2006; 24:5313–5327 [PubMed: 17060676]
6. Poruk KE, Gay DZ, Brown K, et al. The clinical utility of CA 19–9 in pancreatic adenocarcinoma: diagnostic and prognostic updates. Curr Mol Med 2013; 13:340–351 [PubMed: 23331006]
7. Ferrone CR. FOLFIRINOX: desert, oasis, or mirage? Ann Surg Oncol 2015; 22:1059–1060 [PubMed: 25490873]
8. Ganeshan B, Goh V, Mandeville HC, Ng QS, Hoskin PJ, Miles KA. Non-small cell lung cancer: histopathologic correlates for texture parameters at CT. Radiology 2013; 266:326–336 [PubMed: 23169792]
9. Chamming's F, Ueno Y, Ferré R, et al. Features from computerized texture analysis of breast cancers at pretreatment MR imaging are associated with response to neoadjuvant chemotherapy. Radiology 2018; 286:412–420 [PubMed: 28980886]
10. Ng F, Ganeshan B, Kozarski R, Miles KA, Goh V. Assessment of primary colorectal cancer heterogeneity by using whole-tumor texture analysis: contrast-enhanced CT texture as a biomarker of 5-year survival. Radiology 2013; 266:177–184 [PubMed: 23151829]
11. Yip C, Landau D, Kozarski R, et al. Primary esophageal cancer: heterogeneity as potential prognostic biomarker in patients treated with definitive chemotherapy and radiation therapy. Radiology 2014; 270:141–148 [PubMed: 23985274]
12. Yu H, Scalera J, Khalid M, et al. Texture analysis as a radiomic marker for differentiating renal tumors. Abdom Radiol (NY) 2017; 42:2470–2478 [PubMed: 28421244]
13. Eilaghi A, Baig S, Zhang Y, et al. CT texture features are associated with overall survival in pancreatic ductal adenocarcinoma: a quantitative analysis. BMC Med Imaging 2017; 17:38 [PubMed: 28629416]
14. Cassinotto C, Dohan A, Zogopoulos G, et al. Pancreatic adenocarcinoma: a simple CT score for predicting margin-positive resection in patients with resectable disease. Eur J Radiol 2017; 95:33–38 [PubMed: 28987689]
15. Chakraborty J, Langdon-Embry L, Cunanan KM, et al. Preliminary study of tumor heterogeneity in imaging predicts two year survival in pancreatic cancer patients. PLoS One 2017; 12:e0188022 [PubMed: 29216209]
16. Davnall F, Yip CS, Ljungqvist G, et al. Assessment of tumor heterogeneity: an emerging imaging tool for clinical practice? Insights Imaging 2012; 3:573–589 [PubMed: 23093486]
17. Miles KA, Ganeshan B, Hayball MP. CT texture analysis using the filtration-histogram method: what do the measurements mean? Cancer Imaging 2013; 13:400–406 [PubMed: 24061266]
18. Edge SB, Byrd DR, Compton CC, Fritz AG, Greene FL, Trotti A III, eds. AJCC cancer staging manual, 7th ed New York, NY: Springer, 2010
19. Kulkarni NMHD, Hough DM, Tolat PP, Soloff EV, Kambadakone AR. Pancreatic adenocarcinoma: cross-sectional imaging techniques. Abdom Radiol (NY) 2018; 43:253–263 [PubMed: 29128993]
20. Katz MH, Fleming JB, Bhosale P, et al. Response of borderline resectable pancreatic cancer to neoadjuvant therapy is not reflected by radiographic indicators. Cancer 2012; 118:5749–5756 [PubMed: 22605518]
21. Christians KK, Heimler JW, George B, et al. Survival of patients with resectable pancreatic cancer who received neoadjuvant therapy. Surgery 2016; 159:893–900 [PubMed: 26602840]
22. Evans DB, Rich TA, Byrd DR, et al. Preoperative chemoradiation and pancreaticoduodenectomy for adenocarcinoma of the pancreas. Arch Surg 1992; 127:1335–1339 [PubMed: 1359851]
23. Versteijne E, Vogel JA, Besselink MG, et al.; Dutch Pancreatic Cancer Group. Meta-analysis comparing upfront surgery with neoadjuvant treatment in patients with resectable or borderline resectable pancreatic cancer. Br J Surg 2018; 105:946–958 [PubMed: 29708592]
24. Fukukura Y, Takumi K, Higashi M, et al. Contrast-enhanced CT and diffusion-weighted MR imaging: performance as a prognostic factor in patients with pancreatic ductal adenocarcinoma. Eur J Radiol 2014; 83:612–619 [PubMed: 24418286]

25. Yun G, Kim YH, Lee YJ, Kim B, Hwang JH, Choi DJ. Tumor heterogeneity of pancreas head cancer assessed by CT texture analysis: association with survival outcomes after curative resection. Sci Rep 2018; 8:7226 [PubMed: 29740111]

26. Chatterjee D, Katz MH, Rashid A, et al. Histologic grading of the extent of residual carcinoma following neoadjuvant chemoradiation in pancreatic ductal adenocarcinoma: a predictor for patient outcome. Cancer 2012; 118:3182–3190 [PubMed: 22028089]

27. Wang ZJ, Behr S, Consunji MV, et al. Early response assessment in pancreatic ductal adenocarcinoma through integrated PET/MRI. AJR 2018; 211:1010–1019 [PubMed: 30063366]

28. Garces-Descovich A, Morrison TC, Beker K, Jaramillo-Cardoso A, Moser AJ, Mortele KJ. DWI of pancreatic ductal adenocarcinoma: a pilot study to estimate the correlation with metastatic disease potential and overall survival. AJR 2019; 212:323–331 [PubMed: 30667305]

29. Lubner MG, Stabo N, Lubner SJ, et al. CT textural analysis of hepatic metastatic colorectal cancer: pre-treatment tumor heterogeneity correlates with pathology and clinical outcomes. Abdom Imaging 2015; 40:2331–2337 [PubMed: 25968046]

30. Berenguer R, Pastor-Juan MDR, Canales-Vázquez J, et al. Radiomics of CT features may be nonreproducible and redundant: influence of CT acquisition parameters. Radiology 2018; 288:407–415 [PubMed: 29688159]

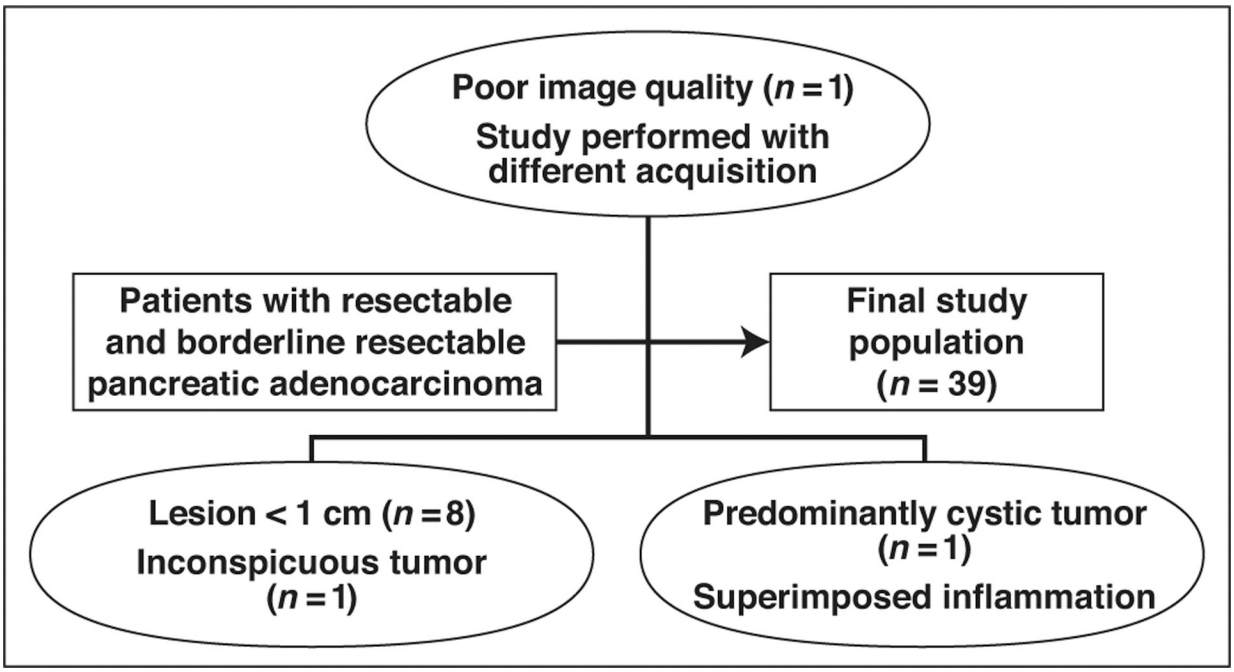

Fig. 1-
Flowchart shows patient selection and exclusion criteria.

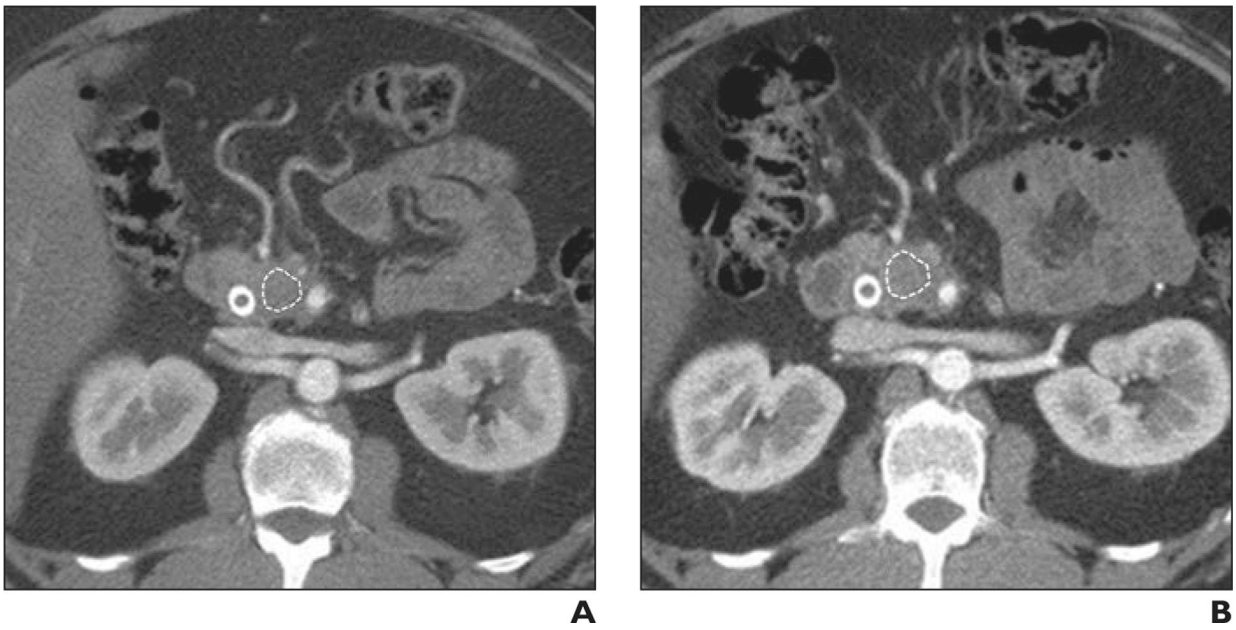

Fig. 2-

Favorable response to neoadjuvant treatment in 53-year-old man.

A and **B,** Axial CT images through pancreatic head obtained during late arterial (pancreatic) phase before (**A**) and after (**B**) neoadjuvant chemotherapy. Polygonal ROI (*outline*) is placed inside largest cross section of tumor for image analysis. No appreciable change in size and degree of vascular involvement was noted on CT. Patient had Evans grade III pathologic response (> 90% tumoral cell destruction) and his cancer antigen 19–9 level had normalized after chemotherapy.

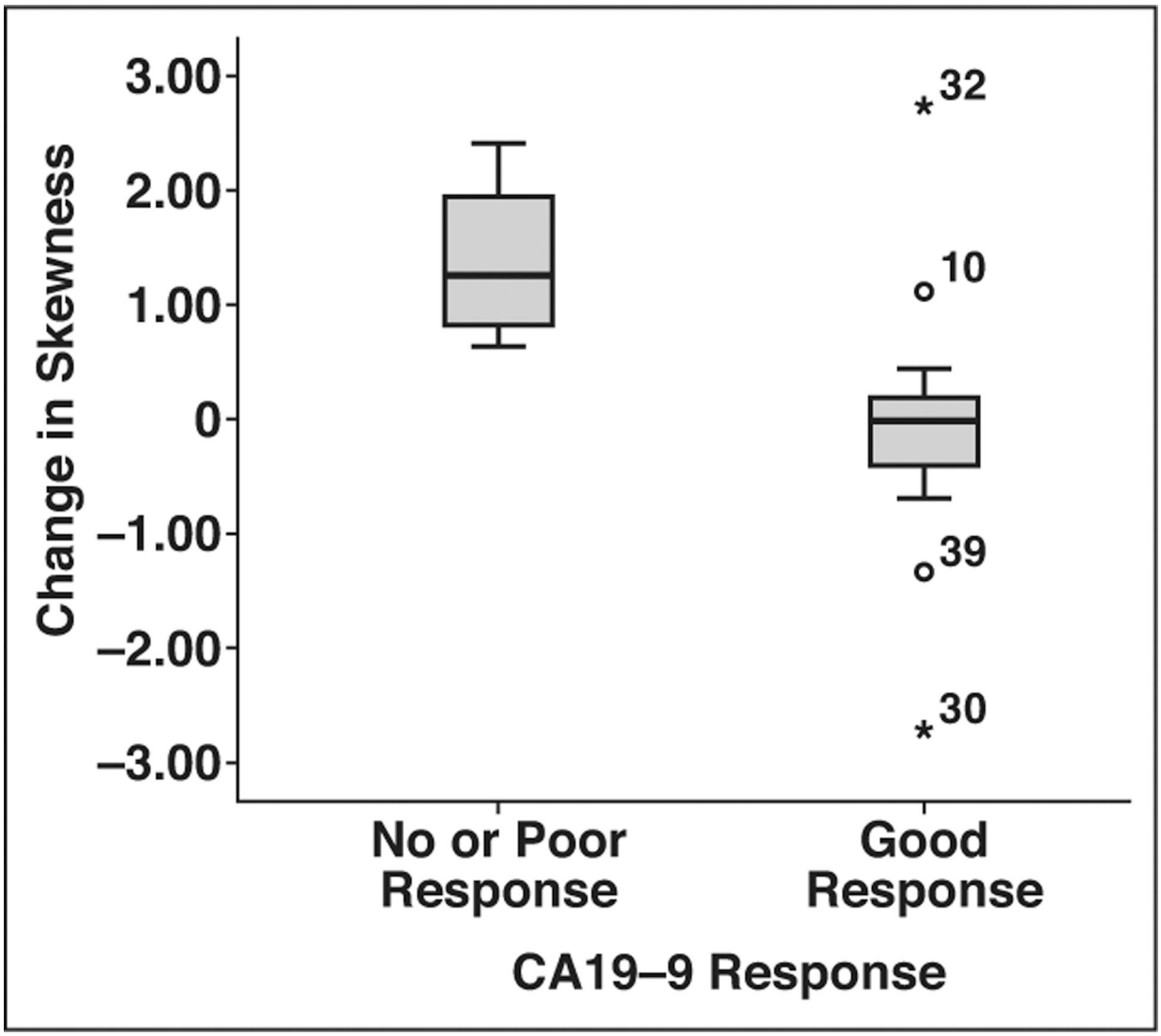

Fig. 3-

Box-and-whisker plot shows correlation between change in skewness (on medium-level filtration) and biochemical response (defined as > 50% drop in cancer antigen [CA] 19–9 level after neoadjuvant chemotherapy) ($p = 0.007$). Upper and lower limits of whiskers represent 2nd and 98th percentiles; circles and asterisks indicate outliers with corresponding patient numbers.

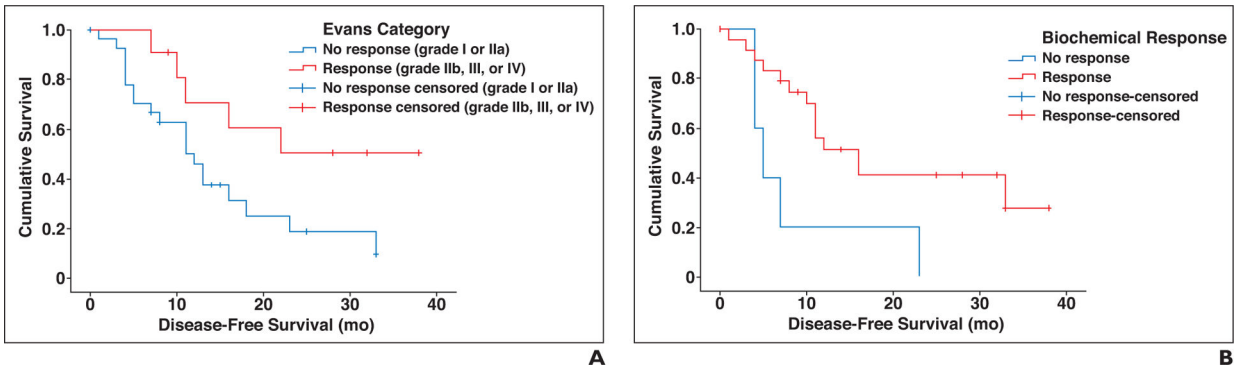

Fig. 4-

Kaplan-Meier survival curves show significant difference in disease-free survival on basis of Evans category (**A**) and biochemical response (**B**).

TABLE 1:

Definition of Evans Criteria for Grading of Pathologic Response

Grade	Histologic Appearance	Categoric Classification
I	Little (< 10%) or no tumor cell destruction	Unfavorable response
IIA	Destruction of 10–50% of tumor cells	Unfavorable response
IIB	Destruction of 51–90% of tumor cells	Favorable response
III	Destruction of > 90% of tumor cells	Favorable response
IV	No viable tumor cells present	Favorable response

Note-Data obtained from [22]. Categoric classification column is binary categoric classification of Evans grades for purpose of nonparametric statistical analysis.

AJR Am J Roentgenol. Author manuscript; available in PMC 2021 February 01.

TABLE 2:

Characteristics of Study Population

Characteristic	All (n = 39)	Type of Response		*p*
		Unfavorable	Favorable	
Sex				1
Female	19	14 (74)	5 (26)	
Male	20	14 (70)	6 (30)	
Age (y)				0.094
Median	67	64	73	
Range	37–80	37–80	54–79	
Tumor size (cm)				0.168
Median	2.8	2.95	2.5	
Range	1–5	1–5	1.5–4.2	
Tumor location in the pancreas				0.305
Head or neck	32	24 (75)	8 (25)	
Body	4	3 (75)	1 (25)	
Tail	3	1 (33)	2 (67)	
Neoadjuvant chemotherapy regimen				**0.004**
Gemcitabine and paclitaxel	22	20(91)	2 (9)	
Gemcitabine and paclitaxel with hydroxychloroquine	17	8 (47)	9 (53)	
Type of surgery				0.179
Whipple	32	24 (75)	8 (25)	
Distal	5	2 (40)	3 (60)	
Appleby	2	2 (100)	0 (0)	
AJCC stage				0.126
IB	4	4 (100)	0 (0)	
IIA	10	5 (50)	5 (50)	
IIB	25	19 (76)	6 (24)	
Histologic grade				
2	30	20(67)	10 (33)	0.415
3	8	7 (88)	1 (12)	
4	1	1 (100)	0 (0)	

AJR Am J Roentgenol. Author manuscript; available in PMC 2021 February 01.

Characteristic	All (n = 39)	Type of Response		*p*
		Unfavorable	Favorable	
CA19–9 level (U/mL)				0.163
Median	148.5	129	302.6	
Range	2.3–14,601	2.3–4469	30–14,601	

Note-Parameters with a significant difference ($p < 0.05$) between favorable response and unfavorable response groups are marked in boldface. Values in parentheses are percentages. AJCC = American Joint Committee on Cancer, CA = cancer antigen.

TABLE 3:

Prediction of Histologic Response With Different Texture Parameters at Different Filtration Levels

	Before Treatment					After Treatment			
	Type of Response					Type of Response			
Filter, Texture Feature	Unfavorable	Favorable	Mann-Whitney *U*Value	*p*	AUC (95% CI)	Unfavorable	Favorable	Mann-Whitney *U*Value	*p*
No filter									
Mean	56.13 (22.52)	54.88 (25.78)	142	0.708		56.13 (12.38)	46.79 (23.97)	93	0.119
SD	20.25 (5.02)	19.55 (6.84)	122	0.318		19.58 (4.96)	17.64 (3.83)	110	0.32
Entropy	4.18 (0.23)	4.26 (0.21)	125.5	0.374		4.12 (0.25)	4.03 (0.18)	114.5	0.398
MPP	56.66 (22.23)	54.88 (24.99)	146	0.803		56.75 (11.74)	47.05 (22.92)	93	0.119
Skewness	0.075 (0.19)	0.12 (0.31)	125.5	0.374		0.07 (0.29)	−0.11 (0.21)	95	0.136
Kurtosis	0.005 (0.38)	0.11 (0.31)	137	0.596		0.11 (0.40)	−0.31 (0.65)	90	0.097
Filter 2									
Mean-2	−7.96 (18.39)	−9.07 (18.58)	148	0.851		−10.16 (16.95)	−3.34 (22.84)	101	0.196
SD-2	48.15 (19.03)	54.95 (18.71)	91	**0.049**	**0.705 (0.53–0.88)**	53.5 (22.34)	48.5 (13.25)	110	0.32
Entropy-2	4.86 (0.28)	4.89 (0.2)	135	0.553		4.78 (0.32)	4.65 (0.26)	124	0.596
MPP-2	35.38 (8.7)	43.51(11.21)	72	**0.01**	**0.766 (0.6–0.93)**	38.8 (13.18)	36.97 (14.9)	137	0.921
Skewness-2	−0.08 (1.03)	−0.11 (0.28)	144.5	0.767		−0.28 (0.87)	0.04 (0.52)	98.5	0.169
Kurtosis-2	0.029 (4.95)	−0.01 (0.48)	142.5	0.72		0.45 (3.29)	0.03 (0.84)	108.5	0.296
Filter 3									
Mean-3	−17.69 (33.57)	−10.86 (33.7)	141	0.685		−38.1 (28.57)	−17.22 (47.86)	94	0.127
SD-3	52.15 (31.06)	51.7 (14.12)	123	0.333		65.39 (32.91)	44.95 (16.74)	81	0.05
Entropy-3	4.75 (0.28)	4.84 (0.21)	127	0.399		4.76 (0.37)	4.72 (0.25)	112.5	0.362
MPP-3	32.14 (9.12)	38.97 (12.33)	100	0.092		32.63 (14.31)	33.23 (10.05)	137	0.921
Skewness-3	−0.17 (1.5)	−0.17 (0.45)	140.5	0.674		−0.64 (1.23)	−0.26 (0.69)	104	0.233
Kurtosis-3	0.71 (7.61)	−0.21 (0.9)	86	**0.034**	**0.279 (0.11–0.45)**	0.56(6.24)	−0.08 (1.71)	95	0.136
Filter 4									
Mean-4	−29.52 (47.8)	−12.58(48.09)	126	0.382		−50.85 (43.83)	−30.34 (71.7)	99	0.174
SD-4	60.18 (36.81)	53.02 (18.8)	143	0.731		68.78 (40.11)	52.56 (13.33)	93	0.119
Entropy-4	4.8 (0.32)	4.88 (0.26)	141.5	0.696		4.81 (0.45)	4.57 (0.25)	97.5	0.159
MPP-4	31.1 (15.58)	42.86 (15.15)	80	**0.021**	**0.74 (0.55–0.93)**	30.4 (15.14)	32.07 (14.81)	136.5	0.908
Skewness-4	−0.29 (1.29)	−0.04 (0.53)	114.5	0.218		−0.27 (1)	−0.04 (0.55)	90.5	0.101

AJR Am J Roentgenol. Author manuscript; available in PMC 2021 February 01.

	Before Treatment					After Treatment			
	Type of Response					Type of Response			
Filter, Texture Feature	**Unfavorable**	**Favorable**	**Mann-Whitney *U*Value**	***p***	**AUC (95% CI)**	**Unfavorable**	**Favorable**	**Mann-Whitney *U*Value**	***p***
Kurtosis-4	0.29 (4.48)	−0.45 (1.42)	118	0.261		−0.14 (3.47)	−0.39 (0.87)	115	0.407
Filter 5									
Mean-5	−42.06 (59.23)	−10.1 (61.08)	111	0.18		−65.9 (57.46)	−40.78 (80.65)	98	0.164
SD-5	59.88 (38.29)	52.3 (25.8)	125	0.365		79.1 (37.35)	51.38 (15.7)	89	0.091
Entropy-5	4.85 (0.35)	4.82(0.3)	148	0.851		4.86 (0.47)	4.56 (0.29)	107.5	0.281
MPP-5	32.69 (26.04)	41.53 (22.97)	110.5	0.175		29.5 (18.03)	37.08 (13.61)	110.5	0.328
Skewness-5	−0.28 (0.87)	0.03 (0.58)	113	0.201		−0.1 (0.74)	0.08 (0.53)	98.5	0.169
Kurtosis-5	−0.25 (1.65)	−0.33 (0.89)	140.5	0.674		−0.55 (1.44)	−0.29 (0.87)	116	0.426
Filter 6									
Mean-6	−60.32 (67.11)	−6.83 (72.76)	104	0.119		−72.19 (66.18)	−46.48 (75.93)	98	0.164
SD-6	62.91 (35.38)	44.7 (29.24)	101	0.098		69.02 (31.89)	45.75 (20.63)	90	0.097
Entropy-6	4.89 (0.36)	4.85 (0.35)	127	0.399		4.84 (0.47)	4.52 (0.3)	99	0.174
MPP-6	37.75 (38.98)	35.63 (17.79)	144	0.755		28.06 (25.65)	36.93 (19.27)	107	0.273
Skewness-6	−0.23 (0.75)	0.15 (0.54)	125.5	0.374		0.04 (0.66)	0.16 (0.61)	123.5	0.584
Kurtosis-6	−0.29 (1.3)	−0.34 (0.66)	145.5	0.791		−0.65 (0.95)	−0.17 (0.96)	110	0.32

Note-Parameters with a significant difference ($p < 0.05$) between favorable response and unfavorable response groups are marked in boldface. Values are expressed as medians with SD in parentheses. MPP = mean positive pixel.

TABLE 4:

Univariate and Multivariate Logistic Regression Models for the Probability of Favorable Histologic Response

Variable	Univariate Model	Full Model	Final Model
Chemotherapy regimen	**11.3 (1.98–63.95)**	**14.9 (1.74–127.89)**	**13.5 (1.92–95.0)**
MPP-4	**1.06 (1.002–1.11)**	**1.08 (1.004–1.16)**	**1.06 (1.002–1.12)**
Kurtosis-3	0.60 (0.29–1.23)	0.49 (0.19–1.27)	
MPP-2	**1.1 (1.02–1.21)**		
SD-2	1.03 (0.99–1.06)		

Note-Values are odds ratios with 95% Cis in parentheses; significant predictors are in boldface. MPP-2 and SD-2 were not entered into the full model because of collinearity with MPP-4. MPP = mean positive pixel.